Analysis of masonry structures: review of and recent trends in homogenization techniques[1]

Paulo B. Lourenço, Gabriele Milani, Antonio Tralli, and Alberto Zucchini

Abstract: The mechanics of masonry structures have been underdeveloped for a long time in comparison with other fields of knowledge. Presently, nonlinear analysis is a popular field in masonry research and homogenization techniques play a major role despite the mathematical and conceptual difficulties inherent to this approach. This paper addresses different homogenization techniques available in published literature, aiming at defining a first catalogue and at discussing the advantages and disadvantages of the different approaches. Finally, special attention is given to a micromechanical based model and a model based on a polynomial expansion of the microstress field. These seem promising and accurate strategies for advanced structural analysis.

Key words: masonry, homogenization, limit analysis, finite elements, in-plane loads, out-of-plane loads.

Résumé : L'aspect mécanique des structures en maçonnerie s'est peu développé par rapport à d'autres domaines techniques. L'analyse non linéaire est présentement un domaine populaire de la recherche en maçonnerie et les techniques d'homogénéisation y jouent un rôle important, malgré les difficultés mathématiques et conceptuelles associées à cette approche. Le présent article traite des différentes techniques d'homogénéisation disponibles dans la littérature, vise à définir un premier catalogue et discute des avantages et des inconvénients des différentes approches. Finalement, une attention particulière est accordée à un modèle micromécanique et à un modèle basé sur une extension d'un polynôme du domaine des microcontraintes. Ce sont des stratégies qui semblent prometteuses et précises pour des analyses structurales poussées.

Mots-clés : maçonnerie, homogénéisation, analyse à la limite, éléments finis, charge dans le plan, charge hors plan.

[Traduit par la Rédaction]

1. Introduction

Masonry is a heterogeneous material that consists of units and joints. Units can be bricks, blocks, ashlars, adobes, irregular stones, and others. Mortar can be clay, bitumen, chalk, lime- or cement-based, glue, or others. The huge number of possible combinations generated by the geometry, nature, and arrangement of units as well as the characteristics of mortars raises doubts about the accuracy of the term "masonry." Still, much information can be gained from the study of regular masonry structures, in which a periodic repetition of the microstructure occurs due to a constant arrangement of the units (or constant bond).

The difficulties in performing advanced testing of these types of structures are quite large due to the numerous variations of masonry, the large scatter of in situ material properties, and the impossibility of reproducing it all in a specimen. Therefore, most of the advanced experimental research carried out in the last few decades concentrated in brick–block masonry and its relevance for design. Accurate modelling requires a comprehensive experimental description of the material, which seems mostly available at the present state of knowledge (CUR 1997; Lourenço 1998).

The global field of structural analysis of masonry structures encompasses several different approaches and a comprehensive review is given in Lourenço (2002). The present paper focuses exclusively on the analysis of unreinforced masonry structures making use of homogenization techniques, which has been receiving a growing interest from the scientific community.

A comprehensive review of the current state of the art, aiming at a classification of approaches, and a discussion on advantages and disadvantages of the different techniques is included. To overcome approximations and limitations identified, two powerful approaches are addressed in detail: (*i*) a micromechanical homogenization approach that considers additional internal deformation mechanisms and (*ii*) a polynomial expansion of the microstress field inside an elementary masonry cell.

2. Homogenization theory: basic assumptions

This section briefly recalls the basis of the theory of homogenization applied to masonry structures, with particular emphasis on running bond texture. Consider a masonry wall Ω consisting of the periodic arrangements of masonry

Received 24 September 2006. Revision accepted 27 June 2007. Published on the NRC Research Press Web site at cjce.nrc.ca on 19 December 2007.

P.B. Lourenço.[2] Associate Professor, Department of Civil Engineering, University of Minho, Azurém, 4800-058 Guimarães, Portugal.
G. Milani and A. Tralli. University of Ferrara, Via Saragat 1, 44100 Ferrara, Italy.
A. Zucchini. ENEA, FIS.MET, v. Don Fiammelli, 2, 40129 Bologna, Italy.

Written discussion of this article is welcomed and will be received by the Editor until 31 March 2008.

[1]This article is one of a selection of papers published in this Special Issue on Masonry.

[2]Corresponding author (e-mail: pbl@civil.uminho.pt).

 doi:10.1139/L07-097

units and mortar joints as shown in Fig.1. The periodicity allows one to regard Ω as the repetition of a representative element of volume (REV or elementary cell) Y.

Let $x = [x_1, x_2]$ be a frame of reference for the global description of Ω (macroscopic scale) and $y = [y_1, y_2, y_3]$ be a frame of reference for Y. The Y module is defined as $Y = \omega \times]-t/2; t/2[$, where $Y \in \Re^3$ is the elementary cell and $\omega \in \Re^2$ represents the middle plane of the plate (Caillerie 1984). The ∂Y boundary surface of the elementary cell (see Fig. 1) is defined as $\partial Y = \partial Y_l \cup \partial Y_3^+ \cup \partial Y_3^-$, where $\partial Y_3^{\pm} = \omega \times [\pm t/2]$.

The basic idea of homogenization consists in introducing averaged quantities representing the macroscopic stress and strain tensors (denoted here, respectively, as $\boldsymbol{E}$ and Σ), as follows:

$$[1] \qquad \boldsymbol{E} = <\varepsilon> = \frac{1}{V}\int_Y \varepsilon(\mathbf{u})\, dY \qquad \Sigma = <\boldsymbol{\sigma}> = \frac{1}{V}\int_Y \sigma\ dY$$

where V stands for the volume of the elementary cell, ε and σ stand for the local quantities (stresses and strains, respectively), and <*> is the average operator.

According to Anthoine (1995) and Cecchi et al. (2005), the homogenization problem in the linear elastic range in the presence of coupled membranal and flexural loads, under the assumption of the Kirchhoff-Love plate theory, can be written as follows:

$$[2a] \qquad \mathrm{div}\boldsymbol{\sigma} = \mathbf{0}$$

$$[2b] \qquad \boldsymbol{\sigma} = a(\boldsymbol{y})\varepsilon$$

$$[2c] \qquad \varepsilon = \boldsymbol{E} + y_3\boldsymbol{\chi} + \mathrm{sym}(\mathrm{grad}\,\mathbf{u}^{\mathrm{per}})$$

$$[2d] \qquad \boldsymbol{\sigma}\,\boldsymbol{e}_3 = 0 \ \text{ on } \partial Y_3^+ \text{ and } \partial Y_3^-$$

$$[2e] \qquad \boldsymbol{\sigma}\,\boldsymbol{n} \ \text{ antiperiodic on } \partial Y_l$$

$$[2f] \qquad \mathbf{u}^{\mathrm{per}} \text{ periodic on } \partial Y_l$$

where $\boldsymbol{\sigma}$ is the microscopic stress tensor (microstress), $a(\mathbf{y})$ represents a ω-periodic linear elastic constitutive law for the components (masonry units and mortar), $\boldsymbol{E}$ is the macroscopic in-plane strain tensor, $\boldsymbol{\chi}$ is the out-of-plane strain tensor (curvature tensor), $\mathbf{u}^{\mathrm{per}}$ is a ω-periodic displacement field, $\boldsymbol{e}_3$ is the unit vector normal to the masonry middle plane, and $\boldsymbol{n}$ is the unit vector normal to the internal cell boundary. Equation [2*a*] represents the microequilibrium for the elementary cell with zero body forces, usually neglected in the framework of homogenization.

Furthermore, in eq. [2*c*], the microstrain tensor ε is obtained as a linear combination among macroscopic $\boldsymbol{E}$ and $\boldsymbol{\chi}$ tensors and a periodic strain field. $\boldsymbol{E}$ and $\boldsymbol{\chi}$ tensors are related to the macroscopic displacement field components $U_1(x_1, x_2)$, $U_2(x_1, x_2)$, and $U_3(x_1, x_2)$ by means of the classic relations $\boldsymbol{E}_{\alpha\beta} = (U_{\alpha,\beta} + U_{\beta,\alpha})/2$, with $\boldsymbol{E}_{i3} = 0$, and $\boldsymbol{\chi}_{\alpha\beta} = -U_{3,\alpha\beta}$ with $\chi_{i3} = 0$, $\alpha, \beta = 1, 2$, and $i = 1,2,3$.

Macroscopic homogenized membrane and bending constants, $\boldsymbol{M}$ and $\boldsymbol{N}$, respectively, can be obtained solving the elastostatic problem [2*a–f*] and making use of the classic relations:

$$[3] \qquad \begin{aligned} \boldsymbol{N} &= \langle\boldsymbol{\sigma}\rangle^* &&= \boldsymbol{A}\boldsymbol{E} + \boldsymbol{B}\boldsymbol{\chi} \\ \boldsymbol{M} &= \langle y_3\boldsymbol{\sigma}\rangle^* &&= \boldsymbol{B}^{\mathrm{T}}\boldsymbol{E} + \boldsymbol{D}\boldsymbol{\chi} \end{aligned}$$

where $\boldsymbol{A}$, $\boldsymbol{B}$, and $\boldsymbol{D}$ are the constitutive homogenized plate tensors. Usually, the elementary cell has a central symmetry, hence $\boldsymbol{B} = 0$. As a rule, a solution for the problem given by eqs. [2*a–f*] can be obtained using standard finite element (FE) packages, as suggested for the in-plane case by Anthoine (1995). The governing equations in the nonlinear case are formally identical to eq. [3], provided that a non linear stress–strain law for the constituent materials is assumed.

2.1. Closed-form solutions in the linear elastic range

This section briefly recalls some of the most popular simplified approaches that have appeared in the past in technical literature for obtaining homogenized elastic moduli for masonry. As the elastostatic problem given in eq. [3] cannot be solved in closed form for running bond masonry, several simplifications were assumed to obtain "easily" homogenized elastic moduli.

2.1.1. Two-step approaches

One of the first ideas presented (Pande et al. (1989), Maier et al. (1991)) was to substitute the complex geometry of the basic cell with a simplified geometry, so that a closed-form solution for the homogenization problem would be possible.

In particular, Pande et al. (1989) presented a model in which a two-step stacked system with alternative isotropic layers was considered (Fig. 2). In this way, a so-called "two-step homogenization" was obtained. In the first step, a single row of masonry units and vertical mortar joints were taken into consideration and homogenized as a layered system. In the second step, the "intermediate" homogenized material was further homogenized with horizontal joints to obtain the final material. In this manner, a very simple mechanical system constituted by elastic springs was obtained and explicit formulas based on classical elasticity concepts were presented.

Obviously, this simplification leads to the following:

- An underestimation of the horizontal stiffness of the homogenized material, as no information on the texture (running bond, stack bond, Flemish bond, etc.) is considered. Furthermore, the inability of the model to consider the regular offset of vertical mortar joints belonging to two consecutive layered unit courses results in significant errors in the case of nonlinear analysis
- A homogenized material that is different if the steps of homogenization are inverted (i.e., if bed joints and masonry units are homogenized in the first step).

Following the idea of a multi-step approach, many other models involving different approximations and ingenious assumptions have been sought, with an increasingly large number of papers in recent years (Pietruszczak and Niu

Fig. 1. Elementary cell used in finite element modelling.

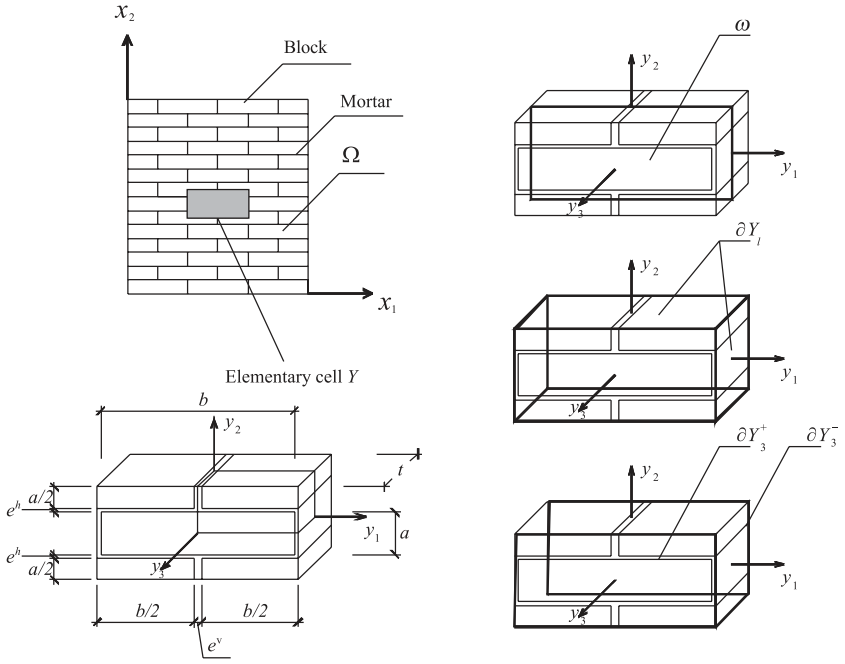

Fig. 2. Two-step homogenization proposed by Pande et al. (1989): (*a*) horizontal homogenization first; (*b*) vertical homogenization first.

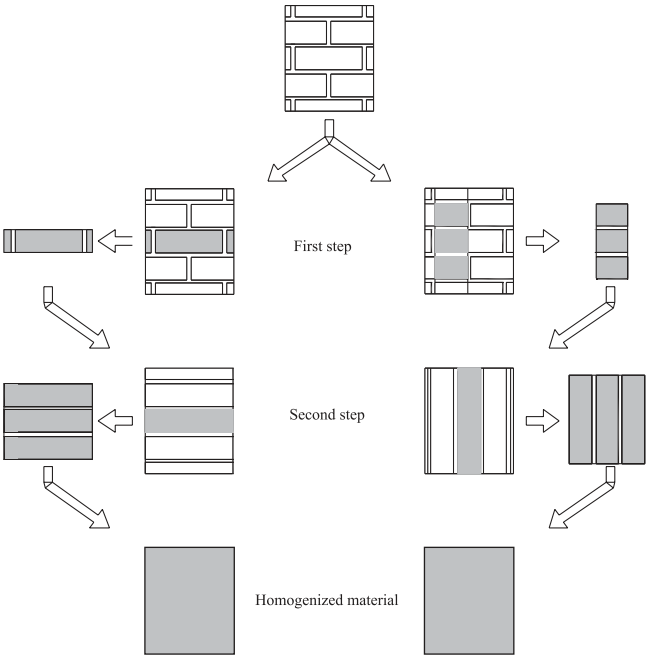

1992), where a two-stage homogenization procedure was employed with the head joints considered as uniformly dispersed elastic inclusions and the bed joints were assumed to represent a set of continuous weakness.

2.1.2. Reduction of joints to interfaces

A different approach, proposed by de Felice (1995) and Cecchi and Sab (2002), is based on the reduction of joints to interfaces. This idea arose from the observation that masonry units are generally much stiffer than mortar and joints have a small thickness when compared with the size of the masonry units.

These studies resulted in the definition of the homogenized masonry constitutive function by means of the introduction of several parameters that measure smallness:

- ε (scale parameter) $\rightarrow 0$, representing the ratio between the size of the cell and the dimension of the overall panel.
- ξ, representing the ratio between the Young's modulus of the mortar, E_m, and the Young's modulus of the masonry unit, E_b ($\xi = E_m/E_b$).
- φ, representing the ratio between the thickness of the joints, e, and the size of the characteristic module a ($\varphi = e/a$).

ξ and φ are parameters that take into account the effects of joint sizes and the ratio of deformability of mortar and block. For fixed elastic tensors of both block and mortar and for fixed geometric parameters *a, b, t* (defined in Fig. 1), the so-called "asymptotic case" is obtained when $\xi \rightarrow 0$ and $\varphi \rightarrow 0$. If φ tends to zero, the joint becomes an interface; whereas, if ξ tends to zero the mortar becomes infinitely deformable with respect to the unit. Therefore, the typology of an asymptotic problem depends on how ξ and φ tend to zero.

A first simplification usually introduced adopts $\xi = \xi(\varphi)$ and $\lim_{\varphi \rightarrow 0} \xi(\varphi)\varphi^{-1} = \rho \neq 0$. Such an asymptotic problem shows cohesive zero thickness interfaces between the masonry units with possible jump of the displacement field. Hence, the field problem may be formulated with reference only to the $\boldsymbol{a}^b$ elastic tensor of the masonry unit with discontinuity at the interfaces, where the constitutive function is a linear relation between the stresses on the unit surfaces and the jump of the displacement field. Both in de Felice (1995) and Cecchi and Sab (2002), elastic springs with diagonal constitutive tensor $\boldsymbol{K}$ for the joints are used, thus introducing a simplification related to the fact that the Poisson effect of

the joint is neglected. In particular $\boldsymbol{K}$ takes the following explicit form:

$$[4] \qquad \boldsymbol{K} = \frac{1}{e}[\mu^{M}\mathbf{I} + (\mu^{M} + \lambda^{M})(\boldsymbol{n}\otimes\boldsymbol{n})]$$

where $\mathbf{I}$ is the identity matrix, $\boldsymbol{n}$ is the normal to the interface, and μ^{M} and λ^{M} are the Lamé constants of mortar.

de Felice (1995) also assumed rigid masonry units, to further reduce the complexity of the problem. In this way (see Fig. 3*a*), this author showed that the problem given by eq. [2*a-f*] can be solved in closed form for running bond masonry and permits analytical formulas for the homogenized elastic constants to be obtained, which depend only on the geometry of the elementary cell and on the mechanical properties of joints.

Following this idea, Cecchi and Sab (2002) proposed a multiparameter homogenization study for the two-dimensional and the three-dimensional (3-D) in-plane case, removing the hypothesis of rigid masonry units (Fig. 3*b*). The finite thickness of the joints was considered in an approximated way only in the constitutive relation of the interfaces. A symbolic FE procedure was adopted, in which the elementary cell was discretized by means of a coarse triangular mesh. Here, the term symbolic is use to indicate that the homogenization problem was handled in symbolic form using a mathematical software. In this way, these authors were able to find "quasi-analytical" formulas.

The disadvantages of this approach are the following:

- The reduction of joints to interfaces, which may strongly reduce the accuracy of the results in the presence of thick mortar joints and ξ ratios tending to zero (Cecchi et al. 2005).
- The introduction of elastic masonry units leads to formulas derived from symbolic FE procedures and does not allow analytical solutions to the homogenization problem.
- A possible development of the method in the nonlinear range can result in nonnegligible errors with respect to FE approaches and experimental evidences, as the role of joint thickness is lost in the simplifications assumed.

2.1.3. Finite element procedures

Anthoine (1995) was the first to suggest the use of standard FE codes for solving the homogenization problem, given by eqs. [2*a–f*], in the case of both stacked and running bond masonry. Anthoine (1995, 1997) and Lourenço (1997*a*) also underlined that homogenized moduli depend on the order of the steps and 3-D effects are always present.

Cecchi et al. (2005) applied FE procedures to out-of-plane loaded and stressed masonry and concluded that:

- Flexural moduli may significantly differ from membrane moduli, especially in the presence of weak mortar joints. As a consequence, Kirchhoff-Love orthotropic homogenized coefficients cannot be obtained simply by integration of membrane moduli.
- Cohesive interface closed-form solutions give unreliable results when the ξ ratio is small.

The classical assumptions adopted in the FE method applied to homogenization are: (*i*) perfect continuity between units and mortar and (*ii*) the periodic displacement that has to be imposed fulfils the constant and (or) linear assumption, at the boundary of the cell of the macroscopic kinematic descriptors $\boldsymbol{E}$ and $\boldsymbol{\chi}$. In this way, considering only a macroscopic strain tensor $\boldsymbol{E}$ acting, suitable boundary conditions (Fig. 4) for $\mathbf{u}^{per}$ periodic and $\boldsymbol{\sigma n}$ antiperiodic on ∂Y_l (which represents the boundary of the module orthogonal to the middle plane) are imposed, meaning that the elastostatic problem can be formulated only on Y. It is worth noting that several engineering approaches recently presented in the technical literature do not satisfy this hypothesis exactly (Lopezç et al. 1999; Zucchini and Lourenço 2002). In this case, the symmetry of the cell allows for simplification of the numerical model and permits to discretize only 1/4 of the elementary cell.

The advantages of the adoption of a FE technique include:

- The FE solution approximates the actual solution for a suitable refined mesh.
- Mortar joints thickness is taken into account for the evaluation of the homogenized moduli, which leads to numerically homogenized moduli estimates that can differ from interface moduli.
- The influence on the homogenized horizontal Young modulus, due to staggering of the masonry units, is caught by the model, especially in the presence of mortar joints with poor mechanical properties or nonlinear behaviour.

On the other hand, the most severe limitation of this approach is that the computational cost of an FE procedure does not compete favourably with macroscopic approaches when nonlinear problems are treated, as the homogenization field problem has to be solved for each Gauss point of each loading step. This leads to the continuous handling of a "two-size" FE problem (macroscopic and cell level), where the averaged results obtained at a cell level are utilized at a structural level (in the framework of a nonlinear numerical procedure).

2.2. Homogenization in the inelastic range

This section briefly reviews the most disseminated nonlinear approaches based on homogenization presented in recent technical literature. As a first attempt, the approaches can be classified as: (*i*) engineered approaches based on continuum models for components or on mortar joint failure, (*ii*) kinematic and static limit analysis approaches, and (*iii*) FE nonlinear analyses.

2.2.1. Engineered approaches

The approaches based on a two-step homogenization procedure have also been expanded to the nonlinear field, including a cracking model (Lee et al. 1996), a damage model (Maier et al. 1991), and a plasticity model (Lourenço 1996*b*).

To overcome the limitations of the two-step homogenization procedure, micromechanical homogenization approaches that consider additional internal deformation mechanisms have been derived, independently, by van der Pluijm (1999), Lopez et al. (1999), and Zucchini and Lourenço (2002).

Other approaches (Luciano and Sacco 1997; Gambarotta and Lagomarsino 1997; Calderini and Lagomarsino 2006) are based on the observation that, in general, masonry failure occurs with the damage of mortar joints, e.g., with crack-

Fig. 3. Elementary cell used in the interface models: (*a*) zero thickness of mortar joints; (*b*) finite thickness of mortar joints.

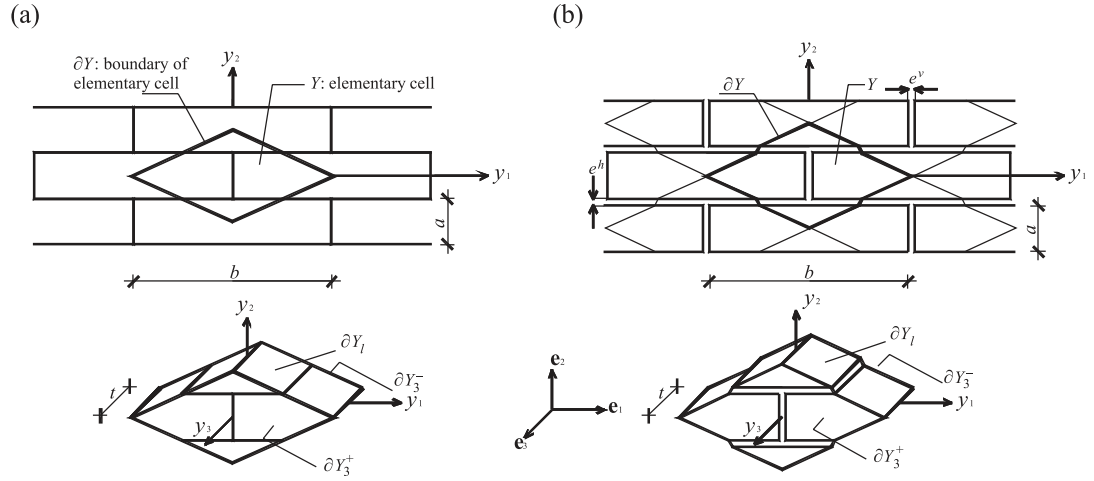

Fig. 4. Applied displacement boundary conditions on the elementary cell.

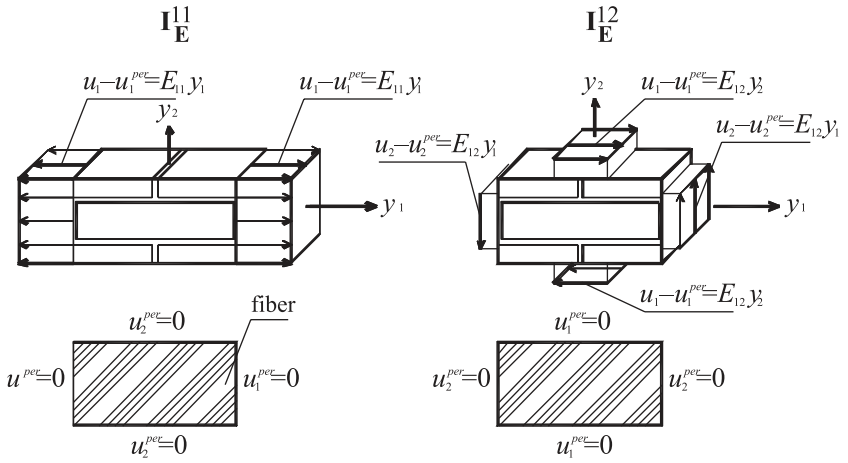

ing and shearing. In this way, masonry failure could occur as a combination of bed and head joints failures (Fig. 5).

The engineered approach has the following advantages: (*i*) its implementation in standard macroscopic FE nonlinear codes is particularly simple and (*ii*) it can compete favourably with macroscopic approaches (Lourenço et al. 1998; Lourenço 2000).

On the other hand, some limitations are worth noting: (*i*) each joint is assumed to be subjected to uniform stress and strain states—more refined analyses, for instance, using more elements along a joints length, could result in a different behaviour of the elementary cell; (*ii*) there is a possibility of unexpected behaviour for load paths and (or) failure mechanisms not explicitly considered in the model.

2.2.2. Limit analysis approaches

Limit analysis approaches (de Buhan and de Felice 1997; Milani et al. 2006*a*, 2006*c*) are based on the assumption of a perfectly plastic behaviour with an associated flow rule for the constituent materials. In this framework, Suquet (1983) proved that both static and kinematic approaches can be used to obtain an upper- or lower-bound estimation of the homogenized failure surface of a periodic arrangement of rigid plastic materials.

de Buhan and de Felice (1997) were the first to apply the kinematic theorem of limit analysis in the framework of masonry homogenization, assuming joints are reduced to interfaces with a classic Mohr-Coulomb failure criterion and masonry units are infinitely resistant.

Milani et al. (2006*a*, 2006*c*) adopted a static approach, in which polynomial equilibrated and admissible stress fields were a-priori assumed in a finite number of subdomains. In this way, both compressive failure and actual thickness of the joints, as well as unit crushing, were considered.

These approaches have the following advantages:

- Masonry homogenized failure surfaces can be recovered by making use of well-known linear programming routines that require a very limited computational effort.
- The homogenized failure surfaces so obtained can be implemented in FE limit analysis codes for collapse analysis without limitations and are not required to solve a cell problem in each Gauss point at a structural level.
- They can compete favourably with macroscopic approaches and give relevant information at failure.

Some of the limitations of these approaches are worth noting:

- Limit analysis is incapable of giving information on displacements at collapse.
- As experimental evidences show, frictional behaviour is typically nonassociated and, at present, mathematical theo-

Fig. 5. Simplified nonlinear approach with joints failure only, damaged state of joints near collapse.

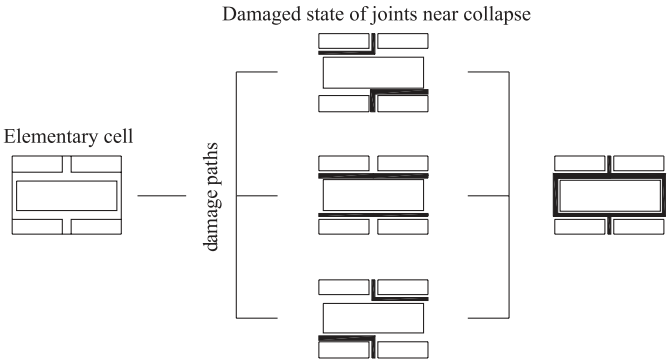

rems concerning nonassociated limit analysis applied to homogenization are not available.

- Masonry behaviour can be quasi-brittle. As a consequence, the assumption of infinite ductility for the constituent materials can be inadequate and can preclude the models to be predictive.

2.2.3. Finite element nonlinear approaches

Today, the increased capabilities of personal computers allow for analyses to be performed in the inelastic range by means of refined discretizations of the elementary cell, using a so-called "multi-level" approach.

The basic idea of a multilevel approach is to solve a nonlinear FE problem at a cell level and to use the microscopic information so obtained at a structural level. In general, an explicit macroscopic constitutive relation for masonry is not obtainable using homogenization, thus implicit approaches have been recently proposed by Pegon and Anthoine (1997) and Massart et al. (2004). In both cases, a nonlinear damage model for the constituent materials has been adopted. In the microscopic step, the Gauss points stress–strain relation is obtained by solving the homogenization problem at a cell level, whereas in the macroscopic step, the structural nonlinear problem is tackled using the Gauss points information collected in the microscopic phase.

In general, these approaches have the following advantages:

- Inelastic masonry behaviour under complex load combinations can be easily followed and is well reproduced, even in the post-peak range.
- The computational cost at a cell level is relatively low and experimental bi-axial failure tests can be fitted with sufficient accuracy, as shown by Massart (2003).
- Real-scale panels of relatively small dimensions can be numerically tested and accurate information at failure is given.

On the other hand, some limitations are worth noting:

- The double computational effort due to the existence of a micro and macroscale mesh does not allow for study of real complex structures and (or) entire 3-D buildings.
- A comparison between computational cost of homogenization with respect to a macroscopic approach shows that the latter is, at present, preferable for the nonlinear analysis of moderately complex structures.

2.3. Application to design practice

Nonlinear analysis represents the most sophisticated tool for structural analysis, capable of predicting the full response from early linear elastic behaviour, through cracking and crushing with associated stress redistributions, followed by ultimate load and definition of a collapse mechanism, up to post-peak behaviour and associated robustness.

The techniques addressed here focus mostly on unreinforced masonry, which still represents a considerable challenge for design, in the case of new structures in moderate seismicity regions, and for assessment, in the case of existing buildings. In these cases, it is widely recognized (Lourenço 2002; Magenes 2006) that linear elastic analysis can hardly be used. Nonlinear analysis, either with rigid block analysis or simplified pushover techniques, now seems to be the appropriate framework for the design of new structures and strengthening measures. In these cases, homogenization techniques represent a significant contribution for modern practice, allowing for the validation and proposition of simple nonlinear nonlin design techniques and solutions for engineering applications. Obviously, the mathematical complexity of the formulations and the required knowledge of masonry mechanics indicate that the techniques addressed will be used by a reduced number of qualified experts.

Finally, it is noted that, from the viewpoint of FE analysis, the possible consideration of reinforced masonry is straightforward, as the mesh reinforcement contribution is simply added to the unreinforced masonry contribution. Nevertheless, it is believed that the practical application of sophisticated nonlinear techniques for reinforced masonry structures is of less relevance.

3. Homogenization theory: basic assumptions

For the purpose of understanding the internal deformational behaviour of masonry components (units and mortar) when average deformations occur on the boundaries of the basic cell, detailed FE calculations can be carried out. For a clear discussion of the internal distribution of stresses, a right-oriented *x*-*y*-*z* coordinate system is defined, where the *x*-axis is parallel to the bed joints, the *y*-axis is parallel to the head joints, and the *z*-axis is normal to the masonry plane.

Figure 6 illustrates the deformation corresponding to the analysis of the basic cell under compression along the *x*-axis, and under shear in the planes *xy*, *xz*, and *yz*. Loading is applied with adequate tying of the nodes in the boundaries, making use of the symmetry and antisymmetry conditions appropriate to each load case. Therefore, the resulting loading might not be associated with uniform stress conditions or uniform strain conditions. Linear elastic behaviour is assumed in all cases.

Figure 6*a* demonstrates that, for compression along the *x*-axis, the unit and the bed joint are mostly subjected to normal stresses, the bed joint is strongly distorted in shear, and the cross joint is subjected to a mixed shear–normal stress action. Figure 6*b* demonstrates that, for *xy* shear, the unit and the head joint are mostly subjected to shear stresses, the bed joint is strongly distorted in the normal direction (tension), and the cross joint is subjected to a mixed shear–normal stress. Due to antisymmetric conditions, the neigh-

Fig. 6. Deformed configuration resulting from the finite element analysis on the basic cell: (*a*) compression *x*, (*b*) shear *xy*, (*c*) shear *xz*, and (*d*) shear *yz* (parts *b–d* from Zucchini and Lourenço 2002).

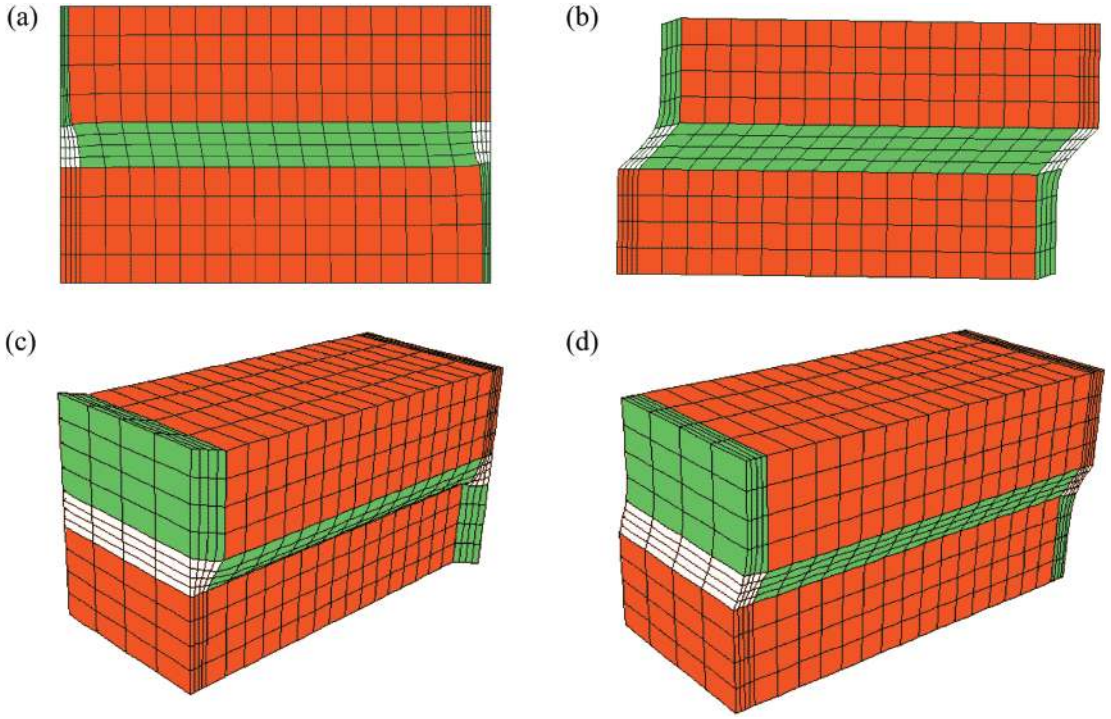

Fig. 7. Adopted geometry symbols (adapted from Zucchini and Lourenço 2002).

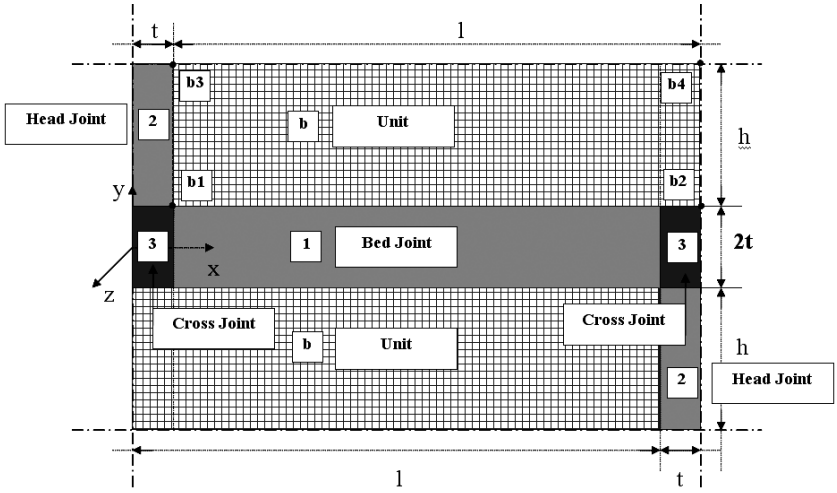

bouring basic cells will feature normal compression in the bed joint.

The deformation of the basic cell under *xz* shear is shown in Fig. 6*c*. The cell components are mostly subjected to shear stresses, with unit and head joint deformed in the horizontal plane, whereas the bed joint is also distorted in the vertical plane. Therefore, the shear stress cannot be neglected in a micromechanical model. Finally, the deformation of the basic cell under *yz* shear is shown in Fig. 6*d*. All cell components are mainly distorted by shear in the vertical plane, whereas minor local stress components do not produce significant overall effects.

3.1. Formulation of the model

Zucchini and Lourenço (2002) have shown that the elastic mechanical properties of an orthotropic material equivalent to a basic masonry cell can be derived from a suitable micromechanical model with appropriate deformation mechanisms that take into account the staggered alignment of the units in a masonry wall. The unknown internal stresses and strains can be found from equilibrium equations at the interfaces between the basic cell components, from a few ingenuous assumptions on the kinematics of the basic cell deformation, and by forcing the macrodeformations of the model and of the homogeneous material to contain the same strain energy. This homogenization model has already been extended with good results to nonlinear problems in the case of a masonry cell failure under tensile loading parallel to the bed joint and under compressive loading by Zucchini and Lourenço (2004, 2007).

Fig. 8. Elastic results for the micromechanical model: (*a*) comparison of Young's moduli with finite element analysis (FEA) results for different stiffness ratios; (*b*) comparison with experimental results of Page (1981, 1983) (from Zucchini and Lourenço 2002).

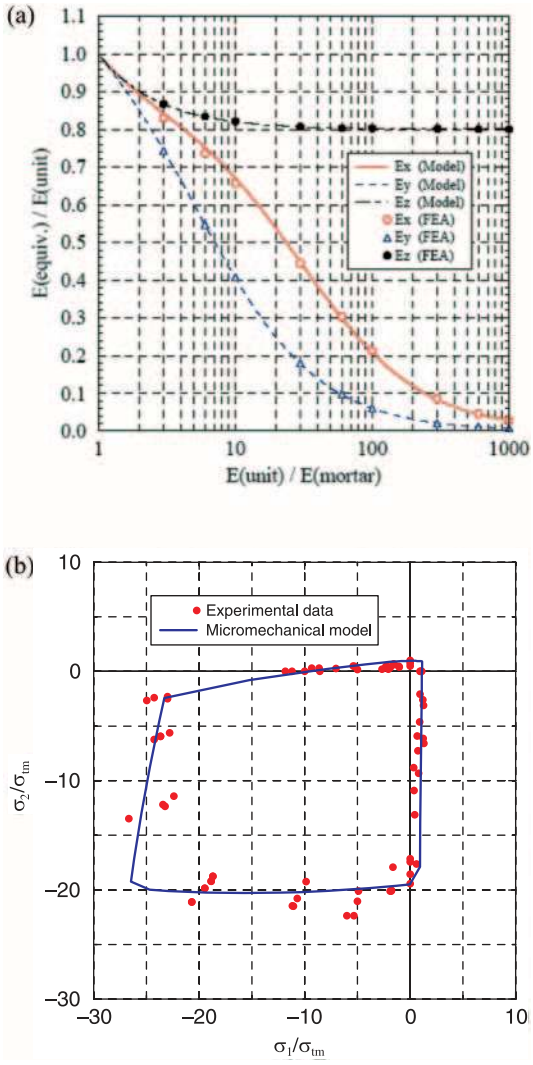

The simulation has been accomplished by coupling the elastic micromechanical model with a damage model for joints and units by means of an iterative solution procedure to calculate the damage coefficients. A simple isotropic damage model with only one single parameter has been used because the discrete internal structure of the cell, and implicitly its global anisotropic behaviour, is taken into account by the 3-D micromechanical model. The geometry for the basic masonry cell and its components is shown in Fig. 7, where it can be seen that the complex geometry is replaced by four components, namely unit, bed joint, head joint, and cross joint.

When the basic cell is loaded only with normal stresses, the micromechanical model of Zucchini and Lourenço (2002) assumes that all shear stresses and strains inside the basic cell can be neglected, except the in-plane shear stress and strain (σ_{xy} and ε_{xy}) in the bed joint and in the unit. The nonzero stresses and strains in the bed joint, head joint, and unit are assumed to be constant, with the exception of the normal stress σ_{xx} in the unit, which is a linear function of x

Fig. 9. Inelastic response of the model in tension: (*a*) infinitely long masonry wall under tensile loading parallel to the bed joints; (*b*) stress–crack opening diagram and comparison with finite element model (FEM) results of Lourenço et al. (1999) (from Zucchini and Lourenço 2004). All dimensions in millimetres.

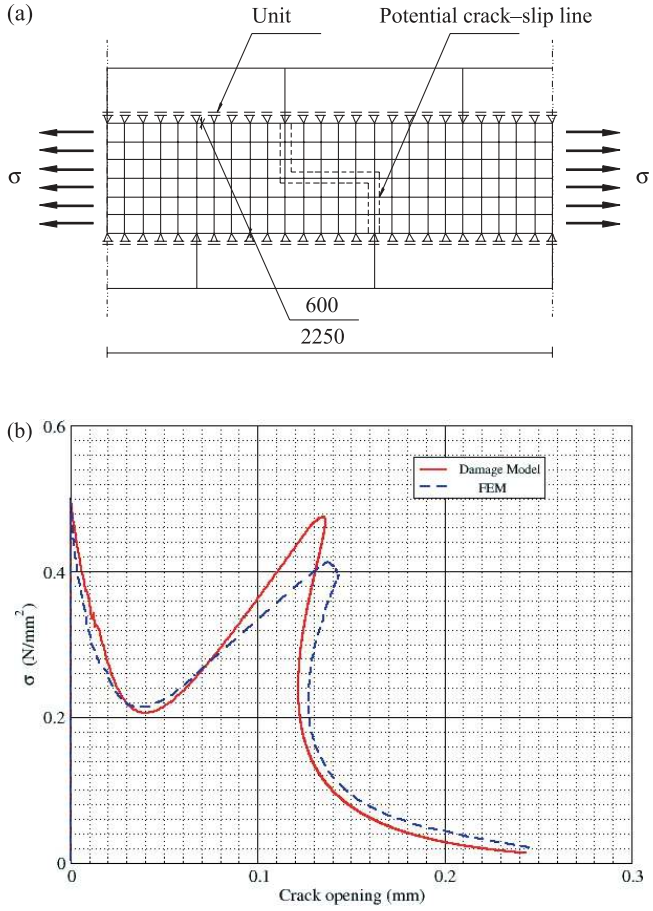

Fig. 10. Axial stress versus axial strain for stronger mortar (prism MU3) (from Zucchini and Lourenço 2007). Comparison between finite element simulation (Lourenço and Pina-Henriques 2006) and nonlinear homogenization model. FEM, finite element model; Hom., homogenization.

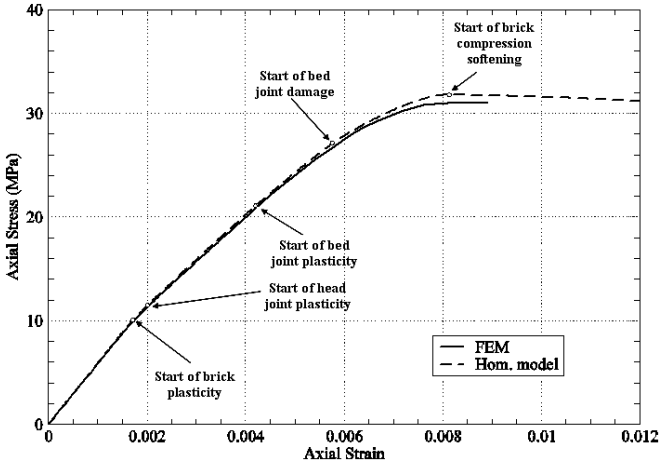

Fig. 11. Periodic structure ($X_1 - X_2$ macroscopic frame of reference) and REV ($y_1 - y_2 - y_3$ local frame of reference).

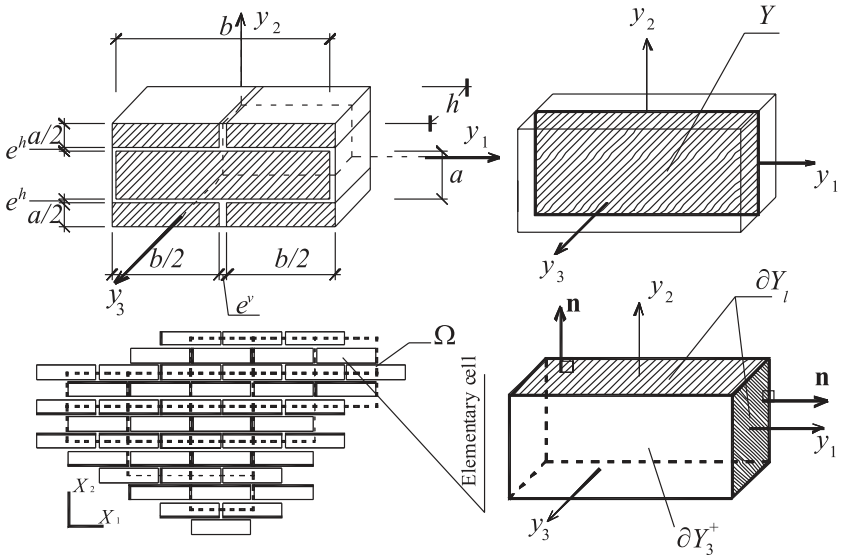

Fig. 12. Stress field polynomial expansion approach. Adopted division in sub-domains: (*a*) subdivision and geometrical characteristics of one-fourth of the elementary cell; (*b*) subdivision into 36 sub-domains for the entire cell.

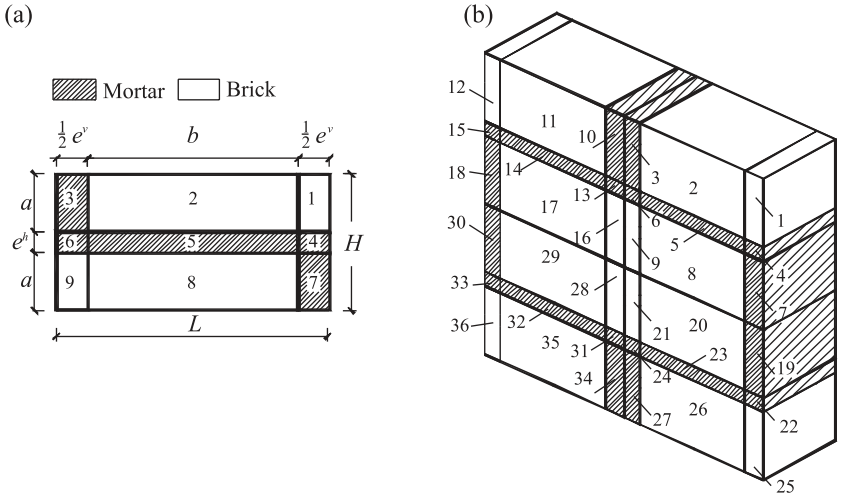

and accounts for the effect of the shear σ_{xy} in the bed joint, and with the exception of the shear stress σ_{xy} in the unit, which is linear in y. The coupling of this model with non-linear constitutive models leads to an iterative algorithm in which, at each cycle, a system of equilibrium equations is solved to obtain the unknown effective stresses and strains.

The governing linear system of 20 equilibrium equations in the unknown internal stresses and strains of the masonry cell, to be solved at each iteration, can be rewritten for a strain-driven compression in y, as:

[5] $$r^2\sigma^2_{xx} = r^{\mathrm{b}}\bar{\sigma}^{\mathrm{b}}_{xx} - \frac{l-t}{2h}r^1\sigma^1_{xy}$$

Interface unit – head joint

[6] $$r^{\mathrm{b}}\sigma^{\mathrm{b}}_{yy} = r^1\sigma^1_{yy}$$ Interface unit – bed joint

[7] $$hr^2\sigma^2_{xx} + 2tr^1\sigma^1_{xx} + hr^{\mathrm{b}}\bar{\sigma}^{\mathrm{b}}_{xx} + (l-t)r^1\sigma^1_{xy} = 0$$

Right boundary

[8] $$\left(h + 4t\frac{r^2}{r^1+r^2}\right)\varepsilon^2_{yy} + h\varepsilon^{\mathrm{b}}_{yy} = 2(h+t)\varepsilon^0_{yy}$$

Upper boundary

[9] $$thr^2\sigma^2_{zz} + \left(l - t + t\frac{r^1+r^2}{r^1}\right)tr^1\sigma^1_{zz} + lhr^{\mathrm{b}}\sigma^{\mathrm{b}}_{zz} = 0$$

Front boundary

[10] $$2t\varepsilon^1_{yy} + h\varepsilon^{\mathrm{b}}_{yy} = \left(4t\frac{r^2}{r^1+r^2} + h\right)\varepsilon^2_{yy}$$

Upper boundary

Fig. 13. Experimental and numerical results from a masonry shear wall: (*a*) principal stress distribution at collapse from the lower bound analysis; (*b*) velocities at collapse from the upper bound analysis; (*c*) comparison between experimental load–displacement diagram and the homogenized limit analysis (lower bound and upper bound approaches).

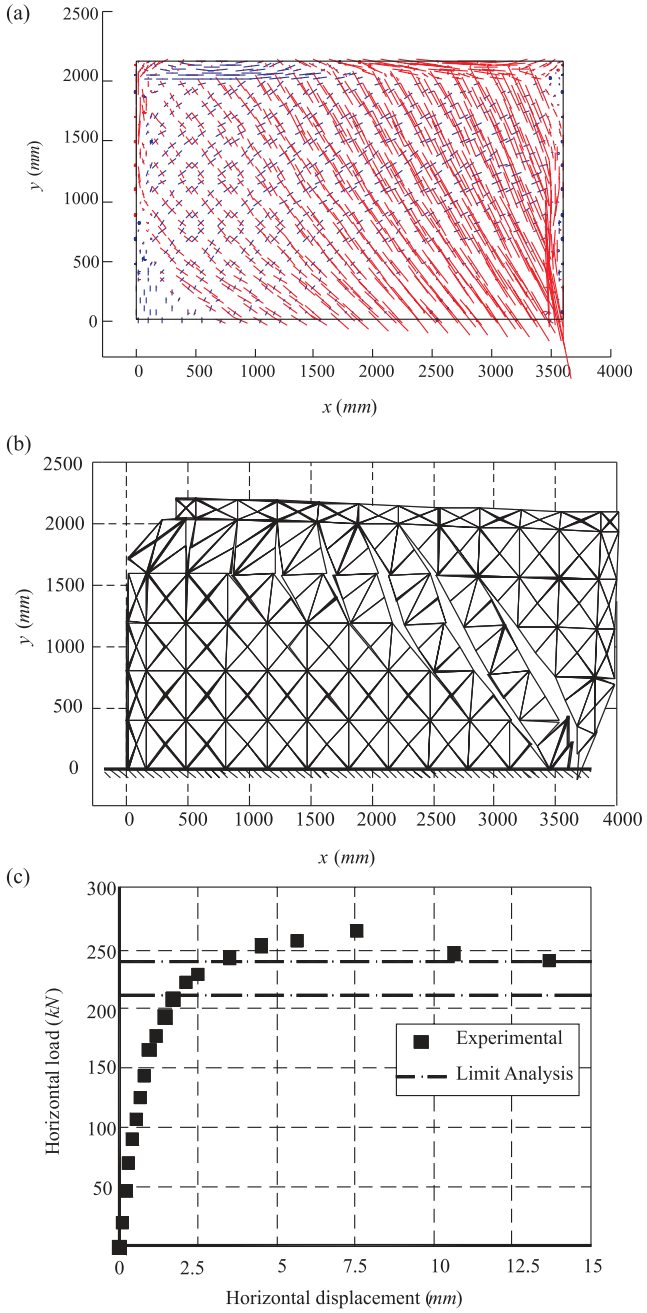

$$[11]\qquad t\varepsilon^2_{xx} + l\bar{\varepsilon}^{\,b}_{xx} = \left(l - t + 4t\frac{r^1}{r^1 + r^2}\right)\varepsilon^1_{xx} \qquad \text{Right boundary}$$

$$[12]\qquad \varepsilon^b_{zz} = \varepsilon^1_{zz} \qquad \text{Front boundary}$$

$$[13]\qquad \varepsilon^b_{zz} = \varepsilon^2_{zz} \qquad \text{Front boundary}$$

$$[14]\qquad \varepsilon^k_{xx} = \frac{1}{E^k}[\sigma^k_{xx} - \nu^k(\sigma^k_{yy} + \sigma^k_{zz})]$$
$$\varepsilon^k_{yy} = \frac{1}{E^k}[\sigma^k_{yy} - \nu^k(\sigma^k_{xx} + \sigma^k_{zz})] \qquad k = b,\ 1,\ 2$$
$$\varepsilon^k_{zz} = \frac{1}{E^k}[\sigma^k_{zz} - \nu^k(\sigma^k_{xx} + \sigma^k_{yy})]$$

$$[15]\qquad \varepsilon^1_{xy} = \frac{\varepsilon^2_{xx} - \bar{\varepsilon}^{\,b}_{xx}}{4} - \left(\frac{l - t}{8hE^b} + \frac{h}{6tG^b}\right)\frac{r^1}{r^b}\sigma^1_{xy}$$

$$[16]\qquad \sigma^1_{xy} = 2G^1\varepsilon^1_{xy}$$

where, as shown in Fig. 7, l is half of the unit length, h is half of the unit height, and t is half of the bed joint width. Here also, $r = 1 - d$, where d is the scalar damage coefficient, ranging from 0 to 1 and representing a measure of the material damage. E is Young's modulus, G is the shear modulus, ν is the Poisson coefficient, ε_{ij} is the strain component, and σ_{ij} is the stress component. Unit, bed joint, and head joint variables are indicated, respectively, by the superscripts b, 1, and 2, according to Fig. 7. $\bar{\sigma}^b_{xx}$ and $\bar{\varepsilon}^b_{xx}$ are the mean value of the (nonconstant) normal stress σ_{xx} and of the (nonconstant) normal strain ε_{xx} in the unit, respectively. ε^0_{yy} is the uniform normal (macro) strain, perpendicular to the bed joint, on the faces of the homogenized basic cell. The damaged stresses $\boldsymbol{\sigma}_d$ and undamaged (or effective) stresses $\boldsymbol{\sigma}$ are correlated by the relation:

$$[17]\qquad \boldsymbol{\sigma}_d = (1 - d)\mathbf{D}\boldsymbol{\varepsilon} = (1 - d)\boldsymbol{\sigma}$$

where $\mathbf{D}$ is the stiffness matrix.

The adopted damage model in tension, Zucchini and Lourenço (2004), is a simple scalar isotropic model with a Rankine type damage surface:

$$[18]\qquad \sigma_p = \sigma_t$$
$$\sigma_t \le \sigma_p \le \infty$$

where σ_p is the maximum effective principal stress and σ_t is the tensile strength of the given cell component. In the unit, where the normal stress σ^b_{xx} varies linearly in the x direction, the damage is controlled by the maximum principal stress in the entire unit and not by the maximum principal stress obtained with the average value $\bar{\sigma}^b_{xx}$.

The damage can only increase monotonically with the evolution law:

$$[19]\qquad d = 1 - \frac{\sigma_t}{\sigma_p}e^{A(1-\sigma_p/\sigma_t)}$$

The parameter A is related to the mode I fracture energy (G^I) and strength (σ_t) of the material by

$$[20]\qquad A_t = \left(\frac{G^I E}{l\sigma_t^2} - \frac{1}{2}\right)^{-1}$$

where l is the characteristic internal length of fracture, usually adopted to obtain mesh independent results, which

is assumed here to be the material dimension in the direction of the load.

The adopted model in compression, Zucchini and Lourenço (2007), is a Drucker–Prager model according to the classical formulation:

$$3k_1\sigma_m + \bar{\sigma} - k_2 = 0 \quad [21]$$

where

$$\sigma_m = \frac{\sigma_{ii}}{3} = -p \quad [22]$$

$$\bar{\sigma} = \sqrt{\frac{1}{2}\sigma'_{ij}\sigma'_{ij}} = \frac{q}{\sqrt{3}}$$

$$k_1 = \frac{2\sin\phi_f}{\sqrt{3}(3-\sin\phi_f)} \quad [23]$$

$$k_2 = \frac{6\cos\phi_f}{\sqrt{3}(3-\sin\phi_f)}c$$

σ_{ii} is the ii stress tensor component, σ'_{ij} is the ij component of the deviatoric stress tensor, ϕ_f is the friction angle, and c is the cohesion. The friction angle was assumed independent from the plastic deformation, while a bi-parabolic law in the strain hardening equivalent plastic strain $\varepsilon_{p,eq}$ is adopted for the material yield stress. The curve $\sigma_c(\varepsilon_{p,eq})$ is completely defined by the material strength σ_{c0} (the peak stress), the peak equivalent plastic strain ε_0, and the post-peak specific fracture energy g_c:

$$\sigma_c = \frac{\sigma_{c0}}{3}\left(-2\frac{\varepsilon_{p,eq}^2}{\varepsilon_0^2} + 4\frac{\varepsilon_{p,eq}}{\varepsilon_0} + 1\right) \qquad 0 \le \varepsilon_{p,eq} \le \varepsilon_0$$

$$\sigma_c = \sigma_{c0}\left\{1 - \left[\frac{2\sigma_{c0}}{3g_c}(\varepsilon_{p,eq} - \varepsilon_0)\right]^2\right\} \qquad \varepsilon_0 \le \varepsilon_{p,eq} \quad [24]$$

3.2. Elastic results

The model described was applied to a real masonry basic cell (bricks dimensions of 210 mm × 100 mm × 52 mm and mortar joints thickness of 10 mm) and compared with the results of an accurate finite element analysis (FEA). The same elastic properties have been adopted for the bed joint, head joint, and cross joint ($E_1 = E_2 = E_3 = E_m$, $\nu_1 = \nu_2 = \nu_m$). Different stiffness ratios between mortar and unit are considered, assuming $E_b = 20$ GPa, $\nu_b = 0.15$ and $\nu_m = 0.15$ as fixed values. The adopted range of E_b/E_m is very large (up to 1000), if only linear elastic behaviour of mortar is considered. However, those high values are indeed encountered if inelastic behaviour is included. In such case, E_b and E_m should be understood as linearized tangent Young's moduli, representing a measure of the degradation of the (tangent and (or) secant) stiffness matrices used in the numerical procedures adopted to solve the nonlinear problem. Note that the ratio E_b/E_m tends to infinity when softening of the mortar is complete and only the unit remains structurally active.

The elastic properties of the homogenized material, calculated by means of the proposed micromechanical model, are compared in Fig. 8*a* with the values obtained by FEA. The agreement is very good in the entire range $1 \le E_b/E_m \le 1000$, with a maximum error ≤ 6%.

A comparison between the results obtained with the micromechanical model and the experimental results of Page (1981, 1983) are given in Fig. 8*b*. Very good agreement is found in the shape of the yield surface, indicating that the proposed model can be used as a possible macromodel to represent the composite failure of masonry.

3.3. Nonlinear results

The eqs. [5]–[24] algorithm was implemented in a numerical program for the simulation of a masonry cell under normal stresses. To check its performance, the algorithm has been tested in the fracture problem of an infinitely long wall under tensile loading parallel to the bed joint (Fig. 9*a*), which has been analysed by Lourenço et al. (1999) with a sophisticated FE interface model based on multisurface plasticity. This model consists of two half units in the vertical direction and two and a half units in the horizontal direction. In the middle of the specimen a potential crack–slip line through head and bed joints is included. The unit dimensions are 900 mm × 600 mm × 100 mm.

The results of the proposed coupled damage–homogenization model are shown in Fig. 9*b*, where they are compared with the FEA of Lourenço et al. (1999) for the case with zero dilatancy angle. The damage model reproduces with good agreement the FEA of the cell degradation and the two peaks of the failure load. The head joint is the first to fail in tension and the bed joint takes its place in the load carrying mechanism of the cell. The load is transferred through bed joint shear from one unit to the other, with the cell showing regained elastic behaviour for increasing loads until final failure of the bed joint in shear. The residual load carrying capacity is zero because there is no vertical compression and, therefore, no friction effect.

The homogenization model was also tested in the simulation up to failure of a basic masonry cell under axial compressive loading perpendicular to the bed joint. For this problem, numerical results are available from the accurate FE calculations of Lourenço and Pina-Henriques (2006) for the case of a masonry cell with solid soft-mud bricks of dimensions 250 mm × 120 mm × 55 mm and mortar joint thickness of 10 mm. These FEAs have been carried out with very detailed meshes either in plane stress, plane strain,

or enhanced plane strain with constant but nonzero normal strains in the out-of-plane direction, the latter being considered the closest possible plane representation of the 3-D behaviour. The nonlinear behaviour of the cell components has been simulated by means of Drucker–Prager plasticity in compression and Rankine model or cracking in tension. Two different types of mortar were taken into consideration, namely weak and strong mortars.

The axial stress versus axial strain curves for one of the analyses (stronger mortar prism) is shown in Fig. 10. The curves obtained with the homogenization model almost coincide with the corresponding FE results in enhanced plane strain, with marginal computational effort and no convergence difficulties. For weak mortars, the plastic flow of the mortar joints starts very early in the loading path, whereas the brick nonlinear behaviour begins a little later. The brick is in a tensioncompression–tension state, while the mortar is in a tri-axial compression state for the lateral containment effect of the stiffer brick. The head joint suffers some negligible damage in tension just before the complete failure of the brick in tension, which leads to the catastrophic failure of the entire cell. For strong mortars, the plastic flow starts earlier in the brick than in the bed joint, due to the higher strength of the mortar. The inversion of the elastic mismatch between mortar and brick in this case (the mortar is much stiffer than the brick) yields a tension–tension–compression state of the bed joint. A substantial (57%) isotropic damage in tension is reached in the bed joint, but the failure of the masonry cell is again driven by the crushing of the brick. The damage of the mortar in the bed is due to the high tension in the x and z direction.

4. A stress field expansion approach

Figure 11 presents a masonry wall Ω constituted by a periodic arrangement of masonry units and mortar disposed in running bond texture, together with a rectangular periodic REV. As shown in a classical paper by Suquet (1983), homogenization techniques combined with limit analysis can be applied for an estimation of the homogenized strength domain S^{hom} of masonry.

In this framework, masonry units and mortar are assumed to be rigid, perfectly plastic materials with associated flow rule. As the lower bound theorem of limit analysis states and under the hypotheses of homogenization, S^{hom} can be derived by means of the following (nonlinear) optimization problem:

$$[25]\qquad S^{\text{hom}} = \left\{ \sum \middle| \begin{cases} \boldsymbol{\Sigma} =< \boldsymbol{\sigma} >= \dfrac{1}{A}\displaystyle\int_Y \boldsymbol{\sigma}\,\mathrm{d}Y & \text{condition a} \\ \operatorname{div}\boldsymbol{\sigma} = \mathbf{0} & \text{condition b} \\ [[\boldsymbol{\sigma}]]\boldsymbol{n}^{\text{int}} = \mathbf{0} & \text{condition c} \\ \boldsymbol{\sigma}\boldsymbol{n} \text{ antiperiodic on } \partial Y & \text{condition d} \\ \boldsymbol{\sigma}(\boldsymbol{y}) \in S^{\text{m}} \quad \forall \boldsymbol{y} \in Y^{\text{m}}\ ; \quad \boldsymbol{\sigma}(\boldsymbol{y}) \in S^{\text{b}} \quad \forall \boldsymbol{y} \in Y^{\text{b}} & \text{condition e} \end{cases} \right\}$$

Here, $[[\boldsymbol{\sigma}]]$ is the jump of microstresses across any discontinuity surface of normal $\boldsymbol{n}^{\text{int}}$ and superscripts m and b represent mortar and brick, respectively. In eq. [25], conditions a and d are derived from periodicity, condition b imposes the microequilibrium, and condition e represents the yield criteria for the components (units and mortar). The averaged quantity representing the macroscopic stress tensors $\boldsymbol{\Sigma}$ is given by:

$$[26]\qquad \boldsymbol{\Sigma} =< \boldsymbol{\sigma} >= \frac{1}{A}\int_Y \boldsymbol{\sigma}\,\mathrm{d}Y$$

where A represents the area of the elementary cell, $\boldsymbol{\sigma}$ represents the local stress quantity, and <*> is the averaging operator.

The proposed solution approach involves a simple and numerically suitable approach for solving the optimization problem. As shown in Fig. 12*a*, 1/4 of the REV is subdivided into nine geometric elementary entities (subdomains), so that all the cell is subdivided into 36 subdomains, as shown in Fig. 12*b*. The subdivision adopted is the coarser one (for 1/4 of the cell) that can be obtained using rectangular geometries for every subdomain. The macroscopic behaviour of masonry strongly depends on the mechanical and geometric characteristics both of units and vertical and horizontal joints. For this reason, the subdivision adopted also seems to be particularly attractive, giving the possibility to separately characterize every component inside the elementary cell. For each subdomain, polynomial distributions of degree m are a priori assumed for the stress components. Since stresses are polynomial expressions, the generic ijth component can be written as follows:

$$[27]\qquad \sigma_{ij}^{(k)} = \boldsymbol{X}(\boldsymbol{y})\boldsymbol{S}_{ij}^{\text{T}} \qquad \boldsymbol{y} \in Y^k$$

where

$$\boldsymbol{X}(\boldsymbol{y}) = [\,1 \quad y_1 \quad y_2 \quad y_1^2 \quad y_1y_2 \quad y_2^2 \quad \ldots\,]$$

$$\boldsymbol{S}_{ij} = [\,S_{ij}^{(1)} \quad S_{ij}^{(2)} \quad S_{ij}^{(3)} \quad S_{ij}^{(4)} \quad S_{ij}^{(5)} \quad S_{ij}^{(6)} \quad \ldots\,]$$

$\boldsymbol{S}_{ij}$ is a vector of length $\widetilde{N}$ defined as

$$\widetilde{N} = \frac{m^2}{2} + \frac{3m}{2} + 1 = \frac{(m+1)(m+2)}{2}$$

and represents the unknown stress parameters, and Y^k represents the kth subdomain.

Cubic interpolation is recommended as an adequate degree for polynomial interpolation of the stress field. Details on equilibrium. antiperiodicity conditions, and validation of the approach are shown in Milani et al. (2006*a*, 2006*b*). Extension of the formulation to out-of-plane behaviour is given in Milani et al. (2006*c*). Here, only validation of the models with structural elements tests is provided.

Fig. 14. Stress field polynomial expansion approach (out-of-plane model). Comparison between numerical results obtained with the present model, numerical results by Lourenço (1997*b*), and experimental data by Chong et al. (1994). Data refer to the University of Plymouth experimental tests (Chong et al. 1994).

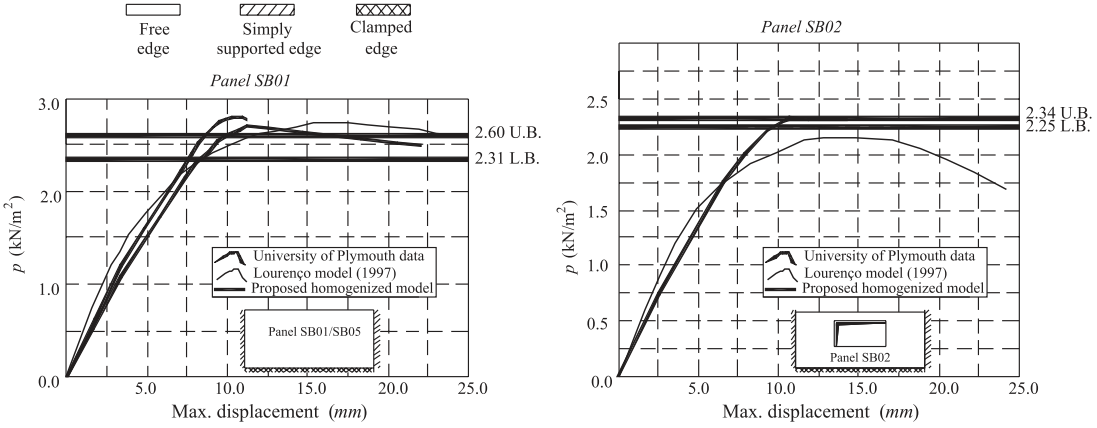

Fig. 15. Typical numerical results (Panel SB02) obtained by means of the stress field polynomial expansion approach (out-of-plane model). (*a*) lower bound results (principal moments at collapse); (*b*) upper bound results (deformed mesh at collapse).

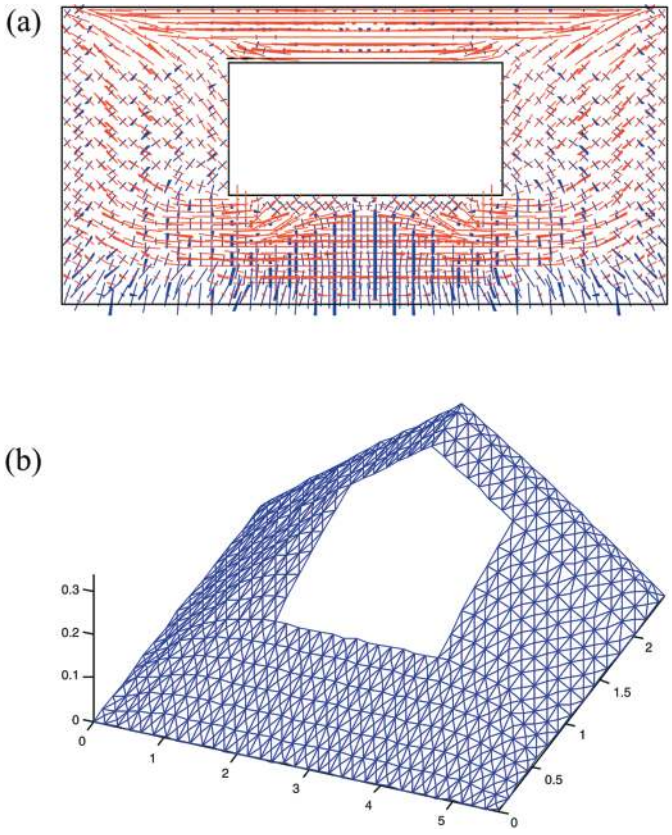

4.1. Numerical results (in-plane)

The homogenized failure surface obtained with the above approach has been coupled with FE limit analysis. Both upper and lower bound approaches have been developed, with the aim to provide a complete set of numerical data for the design and (or) the structural assessment of complex structures. The FE lower bound analysis is based on the equilibrated triangular element by Sloan (1988), whereas the upper bound is based on a modified version of the triangular element with discontinuities of the velocity field in the interfaces by Sloan and Kleeman (1995). The modification takes into account the actual shape of the yield surface for the homogenized material in the interfaces.

Here, the clay masonry shear walls tested by Ganz and Thürlimann (1984) at the Swiss Federal Institute of Technology, ETH Zurich and analysed in Lourenço (1996*a*) is reported. Both for mortar joints and units, a Mohr–Coulomb failure criterion in plane stress is adopted. Experimental evidences show a very ductile response, thus justifying the use of limit analysis for predicting the collapse load, with tensile and shear failure along diagonal stepped cracks.

In Figs. 13*a* and 13*b*, the principal stress distribution at collapse from the lower bound analysis and the velocities at collapse from the upper bound analysis are reported. Finally, in Fig. 13*c*, a comparison between the numerical failure loads are provided, respectively, by the lower and upper bound approaches and the experimental load–displacement diagram is reported. Collapse loads $P(-) = 210$ kN and $P(+) = 245$ kN are numerically found using a model with 288 triangular elements, whereas the experimental failure shear load is approximately $P = 250$ kN.

4.2. Numerical results (out-of-plane)

Milani et al. (2006*c*) further extended and validated the formulation for out-of-plane loading. For this purpose, the elementary cell is subdivided along the thickness in several layers. For each layer, fully equilibrated stress fields are assumed, adopting polynomial expressions for the stress tensor components in a finite number of subdomains, imposing the continuity of the stress vector on the interfaces and defining antiperiodicity conditions on the boundary surface. The out-of-plane failure surfaces of masonry obtained are implemented in FE limit analysis codes (both upper and lower bound) for structural analyses at collapse of entire panels.

The proposed homogenized model is also employed to reproduce experimental data for entire out-of-plane loaded masonry panels. As the current model assumes fully plastic behaviour, simple equilibrium equations (Lourenço 2000) indicate that the experimental values of flexural tensile strength must be divided by three. The panels analyzed here

consist of solid clay brick masonry. The tests were carried out by Chong et al. (1994) and are denoted by SB in Figs. 14 and 15. Four different configurations were tested, built in stretcher bond between two stiff abutments with the vertical edges simply supported (allowance for in-plane displacements was provided) and the top edge free. A completely restrained support was provided at the base because of practical difficulties in providing a simple support. The panels were loaded by air bags until failure with increasing out-of-plane uniform pressure p. The reader is referred to Milani et al. (2006*c*) for a detailed description of panel dimensions, load applications, and results.

Figure 14 shows typical comparisons between experimental pressure–displacement curves by Chong et al. (1994), numerical pressure–displacement curves obtained by means of an orthotropic elasto–plastic macromodel (Lourenço 1997*b*), and the new results with the proposed formulation. In addition, Fig. 15 shows typical results of the numerical analysis in terms of principal moment distribution and mechanisms at failure. The agreement with experimental results is worth noting in all cases analysed.

5. Conclusions

Homogenization techniques represent a popular and active field in masonry research. Several approaches have been recently introduced by different authors and a first attempt to catalogue them and to discuss pros and cons are carried out in this paper. Even if it impossible to predict the future of masonry research, this paper addresses, in detail, two different approaches considered particularly relevant. The first approach is based on micromechanical deformation mechanisms coupled with standard FE analysis. The second approach is based on a polynomial expansion of the stress field coupled with limit FE analysis. It is noted that both approaches include a subdivision of the elementary cell into a high number of different subdomains. In fact, very simplified division of the elementary cell, such as layered approaches, seems inadequate for the nonlinear range.

Homogenized techniques-based structural analysis is probably at a stage when it can start to compete with other structural analysis tools. In the case of FE limit analysis, it seems that failure mechanisms and collapse loads are similar to those obtained by means of more complex approaches based on nonlinear incremental and iterative FE analyses. Such results are obtained at a very small fraction of the effort when compared with the nonlinear simulations.

References

Anthoine, A. 1995. Derivation of the in-plane elastic characteristics of masonry through homogenisation theory. International Journal of Solids and Structures, **32**(2): 137–163. doi:10.1016/0020-7683(94)00140-R.

Anthoine, A. 1997. Homogenisation of periodic masonry: plane stress, generalised plane strain or 3d modelling? Communications in Numerical Methods in Engineering, **13**(5): 319–326. doi:10.1002/(SICI)1099-0887(199705)13:5<319::AID-CNM55>3.0.CO;2-S.

Caillerie, D. 1984. Thin elastic and periodic plates. Mathematical Methods in the Applied Sciences, **6**: 159–191.

Calderini, C., and Lagomarsino, S. 2006. A micromechanical inelastic model for historical masonry. Journal of Earthquake Engineering, **10**(4): 453–479. doi:10.1142/S1363246906002608.

Cecchi, A., and Sab, K. 2002. A multi-parameter homogenization study for modelling elastic masonry. European Journal of Mechanics A-Solids, **21**: 249–268.

Cecchi, A., Milani, G., and Tralli, A. 2005. Validation of analytical multiparameter homogenization models for out-of-plane loaded masonry walls by means of the finite element method. Journal of Engineering Mechanics, **131**(2): 185–198. doi:10.1061/(ASCE)0733-9399(2005)131:2(185).

Chong, V.L., Southcombe, C., and May, I.M. 1994. The behaviour of laterally loaded masonry panels with openings. *In* Proceedings of the 3rd International Masonry Conference, London, 26–28 October 1992. Proceedings of the British Masonry Society, pp. 178–182.

CUR. 1997. Structural masonry: an experimental/numerical basis for practical design rules. *Edited by* J.G. Rots. Balkema, Rotterdam, the Netherlands.

de Buhan, P., and de Felice, G. 1997. A homogenisation approach to the ultimate strength of brick masonry. Journal of the Mechanics and Physics of Solids, **45**: 1085–1104. doi:10.1016/S0022-5096(97)00002-1.

de Felice, G. 1995. Metodi di omogeneizzazione per sistemi regolari di corpi rigidi. *In* Proceedings of the XII AIMETA Congress. Naples, Italy, 3–6 October 1995. University of Naples, Naples, Italy. pp. 453–479. [In Italian.]

Gambarotta, L., and Lagomarsino, S. 1997. Damage models for the seismic response of brick masonry shear walls. Part I: the mortar joint model and its applications. Earthquake Engineering & Structural Dynamics, **26**(4): 423–439. doi:10.1002/(SICI)1096-9845(199704)26:4<423::AID-EQE650>3.0.CO;2-#.

Ganz, H.R., and Thürlimann, B. 1984. Tests on masonry walls under normal and shear loading. Institute of Structural Engineering, ETH Zurich, Zurich, Switzerland. Report No. 7502–4. [In German.]

Lee, J.S., Pande, G.N., Middleton, J., and Kralj, B. 1996. Numerical modelling of brick masonry panels subject to lateral loadings. Computers & Structures, **61**: 735–745. doi:10.1016/0045-7949(95)00361-4.

Lopez, J., Oller, S., Oñate, E., and Lubliner, J. 1999. A homogeneous constitutive model for masonry. International Journal for Numerical Methods in Engineering, **46**(10): 1651–1671. doi:10.1002/(SICI)1097-0207(19991210)46:10<1651::AID-NME718>3.0.CO;2-2.

Lourenço, P.B. 1996*a*. Computational strategies for masonry structures [online]. Ph.D. thesis, Delft University of Technology, the Netherlands. Available from www.civil.uminho.pt/masonry/Publications/1996a_Lourenco.pdf [accessed 10 December 2007].

Lourenço, P.B. 1996*b*. A matrix formulation for the elastoplastic homogenisation of layered materials. Mechanics of Cohesive-Frictional Materials, **1**(3): 273–294. doi:10.1002/(SICI)1099-1484(199607)1:3<273::AID-CFM14>3.0.CO;2-T.

Lourenço, P.B. 1997*a*. On the use of homogenisation techniques for the analysis of masonry structures. Masonry International, **11**: 26–32.

Lourenço, P.B. 1997*b*. An anisotropic macro-model for masonry plates and shells: Implementation and validation. Delft University of Technology, Delft, the Netherlands. Report 03.21.1.3.07.

Lourenço, P.B. 1998. Experimental and numerical issues in the modeling of the mechanical behavior of masonry. *In* International Seminar on Structural Analysis of Historical Constructions II, CIMNE, Barcelona, Spain, 4–6 November 1998. *Edited by* P. Roca et al. International Center for Numerical Methods in Engineering, Barcelona, Spain. pp. 57–91.

Lourenço, P.B. 2000. Anisotropic softening model for masonry plates and shells. Journal of Structural Engineering, **126**(9): 1008–1016. doi:10.1061/(ASCE)0733-9445(2000)126:9(1008).

Lourenço, P.B. 2002. Computations of historical masonry constructions. Progress in Structural Engineering and Materials, **4**: 301–319. doi:10.1002/pse.120.

Lourenço, P.B., and Pina-Henriques, J.L. 2006. Validation of analytical and continuum numerical methods for estimating the compressive strength of masonry. Computers & Structures, **84**: 1977–1989. doi:10.1016/j.compstruc.2006.08.009.

Lourenço, P.B., Rots, J.G., and Blaauwendraad, J. 1998. Continuum model for masonry: parameter estimation and validation. Journal of Structural Engineering, **124**(6): 642–652. doi:10.1061/(ASCE)0733-9445(1998)124:6(642).

Lourenço, P.B., Rots, J.G., and van der Pluijm, R. 1999. Understanding the tensile behaviour of masonry parallel to the bed joints: a numerical approach. Masonry International, **12**: 96–103.

Luciano, R., and Sacco, E. 1997. Homogenisation technique and damage model for old masonry material. International Journal of Solids and Structures, **34**: 3191–3208. doi:10.1016/S0020-7683(96)00167-9.

Magenes, G. 2006. Masonry building design in seismic areas: Recent experiences and prospects from a European standpoint. *In* Proceedings of the First European Conference on Earthquake Engineering and Seismology, Geneva, Switzerland, 3–8 September 2006. [CD-ROM]. Swiss Seismological Service, Zurich, Switzerland. Keynote Address K9.

Maier, G., Papa, E., and Nappi, A. 1991. On damage and failure of unit masonry. *In* Proceedings of the Experimental and Numerical Methods in Earthquake Engineering, Brussels and Luxembourg, 7–11 October 1991. Balkema Editions, Kluwer Academic Publishers, Dordrecht, the Netherlands. pp. 223–245.

Massart, T.J. 2003. Multi-scale modeling of damage in masonry structures. Ph.D. thesis, University of Bruxelles, Belgium.

Massart, T.J., Peerlings, R.H.J., and Geers, M.G.D. 2004. Mesoscopic modeling of failure and damage-induced anisotropy in brick masonry. European Journal of Mechanics A-Solids, **23**: 719–735.

Milani, G., Lourenço, P.B., and Tralli, A. 2006*a*. Homogenised limit analysis of masonry walls, Part I: failure surfaces. Computers & Structures, **84**: 166–180. doi:10.1016/j.compstruc.2005.09.005.

Milani, G., Lourenço, P.B., and Tralli, A. 2006*b*. Homogenised limit analysis of masonry walls, Part II: structural applications. Computers & Structures, **84**: 181–195. doi:10.1016/j.compstruc.2005.09.004.

Milani, G., Lourenço, P.B., and Tralli, A. 2006*c*. Homogenization approach for the limit analysis of out-of-plane loaded masonry walls. Journal of Structural Engineering, **132**(10): 1650–1663. doi:10.1061/(ASCE)0733-9445(2006)132:10(1650).

Page, A.W. 1981. The biaxial compressive strength of brick masonry. *In* Proceedings - Institution of Civil Engineers, Part 2, **71**: 893–906.

Page, A.W. 1983. The strength of brick masonry under biaxial compression-tension. International Journal of Masonry Construction, **3**: 26–31.

Pande, G.N., Liang, J.X., and Middleton, J. 1989. Equivalent elastic moduli for unit masonry. Computers and Geotechnics, **8**(3): 243–265. doi:10.1016/0266-352X(89)90045-1.

Pegon, P., and Anthoine, A. 1997. Numerical strategies for solving continuum damage problems with softening: application to the homogenisation of masonry. Computers & Structures, **64**: 623–642. doi:10.1016/S0045-7949(96)00153-8.

Pietruszczak, S., and Niu, X. 1992. A mathematical description of macroscopic behaviour of brick masonry. International Journal of Solids and Structures, **29**: 531–546. doi:10.1016/0020-7683(92)90052-U.

Sloan, S.W. 1988. Lower bound limit analysis using finite elements and linear programming. International Journal for Numerical and Analytical Methods in Geomechanics, **12**: 61–77. doi:10.1002/nag.1610120105.

Sloan, S.W., and Kleeman, P.W. 1995. Upper bound limit analysis using discontinuous velocity fields. Computer Methods in Applied Mechanics and Engineering, **127**: 293–314. doi:10.1016/0045-7825(95)00868-1.

Suquet, P. 1983. Analyse limite et homogeneisation. Comptes Rendus de l'Académie des Sciences - Series IIB - Mechanics, **296**: 1355–1358. [In French.]

van der Pluijm, R. 1999. Out of plane bending of masonry: behaviour and strength. Ph.D. dissertation, Eindhoven University of Technology, the Netherlands.

Zucchini, A., and Lourenço, P.B. 2002. A micro-mechanical model for the homogenization of masonry. International Journal of Solids and Structures, **39**: 3233–3255. doi:10.1016/S0020-7683(02)00230-5.

Zucchini, A., and Lourenço, P.B. 2004. A coupled homogenisation–damage model for masonry cracking. Computers & Structures, **82**: 917–929. doi:10.1016/j.compstruc.2004.02.020.

Zucchini, A., and Lourenço, P.B. 2007. Mechanics of masonry in compression: results from a homogenisation approach. Computers & Structures, **85**: 193–204. doi:10.1016/j.compstruc.2006.08.054.